Path Planning of AUV Swarms Using a Bio-inspired Multi-Agent System

Sarada Prasanna Sahoo[1], **Bikramaditya Das**[2†], and **Bibhuti Bhusan Pati**[1], Non-members

ABSTRACT

This paper uses a multi-agent system (MAS) as the bioinformatics-inspired technique for guiding a team of autonomous underwater vehicles (AUVs) toward the desired destination. An individual AUV is designated as an agent connected by a communication network and assumes full communication. Here, each AUV estimates the position of its neighbor AUVs while moving toward the destination. The proposed multi-AUV system consists of a leader AUV and five follower AUVs. A distributed path consensus (DPC) is proposed to ensure the neighboring agent AUVs maintain a predefined distance between each other while moving toward the predefined destination. Due to the proposed distance constraint between neighboring agents, AUVs stay at a safe distance from each other while maintaining underwater communication using interactive switching topology. The performance of the optimized path is obtained using MATLAB simulation. The proposed algorithm is applied in both, formation using the desired shape, and trajectory tracking, and found to be globally asymptotically stable. The results of the simulation confirm that each agent switches from one state to another and progress over time until the desired coordinated shape is achieved without inter-vehicular collision. The proposed method solves coordination problems among multiple AUVs and increases the coverage of underwater missions like oceanographic surveys.

Keywords: Autonomous Underwater Vehicle, AUV, Distributed Path Consensus, DPC, Multi-Agent System, MAS, Path Planning, Position Estimation

1. INTRODUCTION

The underwater world is vast and covering a finite area requires the involvement of multiple autonomous underwater vehicles (AUVs) as a team [1]. The path planning of multiple AUVs using the multi-agent system (MAS) is inspired by the team behavior of humans when working toward achieving a common goal within a defined time span [2]. The multi-agent system (MAS) maintains the relative positions and orientations deployed by the team while approaching the destination [3]. Control involving path planning requires a complicated controller design to maintain inter-vehicular communication to avoid collision among the AUVs and with other obstacles [4, 5]. The dynamic underwater environment [6] and unavailability of GPS signals [7] make the performance of path planning control tasks quite challenging. Thus, designing fewer complex controllers for path planning control is recently gaining research interest [8, 9]. Most methods for the path planning control of multiple AUVs advocate the leader-follower structure [3–9], where follower vehicles trace the trajectory of a leader AUV. The leader AUV decides the direction of formation advancement, while follower AUVs maintain the required angle of orientation and position with respect to the path of the leader [10].

Challenges such as the dynamic behavior of the underwater environment and unavailability of GPS signals have been discussed in many previous studies. Different consensus algorithms for managing underwater sensor networks and monitoring underwater scenarios based on MAS have been discussed in [11]. Szymak and Praczyk [12] developed a control system architecture for MAS consisting of AUVs employed in underwater surveys. Yang and Zhang [13] suggested employing Jacobi transform and geometrical reduction techniques to separately design shape, motion, and AUV orientation controllers. Bian *et al.* [14] designed a Discrete Event Dynamic System (DEDS) model of the task planning-based controller to address the distributed formation control problem using MAS with varying communication topology. Hu *et al.* [15] proposed an energy-efficient information exchange triggered by an impulse signal between AUVs in a multi-AUV formation topology. A formation controller and a consensus law for MAS based on position estimation has also been discussed in the literature [16]. The MAS technique is also used for routing underwater acoustic sensor networks [17]. An agent system is proposed for reconfigurable control strategies in switching topology networks [18] and the early detection of aquatic pests [19]. A distributed consensus observer to estimate the state of a leader for a leader-follower formation topology in MAS is discussed in [8]. To address the leader-follower consensus problem, distorted formation shape and steady-state motion of the group are the challenging tasks [20]. Consensus observer is used to estimate the unmeasured states of

Manuscript received on June 2, 2021; revised on December 18, 2021; accepted on January 17, 2022. This paper was recommended by Associate Editor Matheepot Phattanasak.

[1]The authors are with the Department of Electrical Engineering, Veer Surendra Sai University of Technology, Burla, India.

[2]The author is with the Department of Electronics and Telecommunication Engineering, Veer Surendra Sai University of Technology, Burla, India.

[†]Corresponding author: adibik09@gmail.com

Digital Object Identifier: 10.37936/ecti-eec.2022203.247509

$$M_\eta\left(\eta_k\right)\ddot{\eta}_k + C_\eta\left(\eta_k,\dot{\eta}_k\right)\dot{\eta}_k + D_\eta\left(\eta_k,\dot{\eta}_k\right)\dot{\eta}_k + g\left(\eta_k\right) = T_k \tag{1}$$

$$\begin{aligned}
\dot{u} &= \frac{m_{22}}{m_{11}}vr - \frac{X_u}{m_{11}}u - \frac{X_{u|u|}}{m_{11}}u\left|u\right| + \frac{1}{m_{11}}F_u \\
\dot{v} &= -\frac{m_{11}}{m_{22}}ur - \frac{Y_v}{m_{22}}v - \frac{Y_{v|v|}}{m_{22}}v\left|v\right| + \frac{1}{m_{22}}F_v \\
\dot{r} &= \frac{m_{11}-m_{22}}{m_{33}}uv - \frac{N_r}{m_{33}}r - \frac{N_{r|r|}}{m_{33}}r\left|r\right|
\end{aligned} \tag{2}$$

$$\dot{\nu} = \begin{bmatrix} -\frac{X_u}{m_{11}} - \frac{X_{u|u|}}{m_{11}}\left|u\right| & \frac{m_{22}}{m_{11}}r & 0 \\ -\frac{m_{11}}{m_{22}}r & -\frac{Y_v}{m_{22}} - \frac{Y_{v|v|}}{m_{22}}\left|v\right| & 0 \\ \frac{m_{11}-m_{22}}{m_{33}}v & 0 & -\frac{N_r}{m_{33}} - \frac{N_{r|r|}}{m_{33}}\left|r\right| \end{bmatrix}\begin{bmatrix} u \\ v \\ r \end{bmatrix} + \begin{bmatrix} \frac{1}{m_{11}} & 0 \\ 0 & \frac{1}{m_{22}} \\ 0 & 0 \end{bmatrix} F \tag{3}$$

a given leader system for each agent in a distributed fashion to address the communication loop problem [21]. To overcome the disadvantages discussed above, the distributed path consensus (DPC) algorithm is used for path planning using bio-inspired MAS. Bhattacharya *et al.* [22, 23] developed a DPC algorithm for use in the path planning and task assignment of MAS but not the underwater environment. Based on the literature, no proof is available on the fixed symmetric topology of directed graph research. Therefore, the stability proof for multi-agent systems subject to directed topology is nontrivial and quite challenging.

This paper deals with the path planning of coordinated multiple AUVs using switching topology based on the concept of bio-inspired MAS. MAS is proposed to estimate the position of the various AUVs in the underwater environment relative to each other by considering their relative position. Here, each agent is represented by an AUV connected by a communication graph network [24, 25]. All the AUVs are assumed to be identical. The position estimation method is proposed to determine the positions of neighbor agent AUVs for path planning and optimization. The DPC is proposed for path optimization by implementing a distance constraint that ensures a predefined distance between the neighboring AUVs while moving toward the destination. The resultant distance constraint of the proposed algorithm maintains a safe distance from each agent AUV while communicating among themselves. Path optimization is performed separately for each AUV to determine the minimum cost route between the start and destination point.

The contributions of this paper are as follows:

- A MAS controller is proposed based on position estimation to obtain the desired shape while approaching the destination.
- The proposed controller avoids inter-AUV collision while prevailing communication and provides an optimized path.
- Stability analysis of the proposed algorithm is obtained using the Lyapunov stability theorem.
- The performance based on tracking error in the X and Y direction is verified through MATLAB simulation.

This paper is organized into the following sections: Problem formulation and communication consensus are presented in Sections 2 and 3, respectively. Section 4 explains the proposed position controller design and DPC algorithm. The simulation results are analyzed in Section 5, and the research conclusion is presented in Section 6.

2. PROBLEM FORMULATION

The nonlinear AUV model in an inertial frame can be expressed as Eq. (1) [1], with $\dot{\eta}_k = R\left(\psi_k\right)V_k$, where $\eta_k = \left[x_k, y_k, z_k, \phi_k, \theta_k, \psi_k\right]^T$ is the position matrix, $V_k = \left[u_k, v_k, w_k, p_k, q_k, r_k\right]^T$ is the velocity matrix, T_k is the matrix of force and moments, and $V_k \in R^k$, $\eta_k \in R^k$, $T_k \in R^k$. Further details of the system dynamics can be found in [1]. The dynamics for a AUV with 2D planes of symmetry is expressed by the differential equations in Eqs. (2) and (3) [1], where

$$\dot{\nu} = \begin{bmatrix} \dot{u} \\ \dot{v} \\ \dot{r} \end{bmatrix}, \quad T = \begin{bmatrix} F_u \\ F_v \end{bmatrix}. \tag{4}$$

The parameters m_{11}, m_{22} are the combined rigid body and added mass terms along the xb-axis and yb-axis, respectively [1]. m_{33} is the combined rigid body and added moment of inertia along zb-axis. The variables F_u and F_v denote the control force along the surge and sway motion, respectively. $X_u X_{u|u|}$ are added masses while X_u, Y_v, N_r represent surge linear drag, sway linear drag, and yaw linear drag coefficients, respectively, which are taken as model parameters. Similarly, $X_{u|u|}$, $Y_{v|v|}$, $N_{r|r|}$ represent surge quadratic drag, sway quadratic drag, and

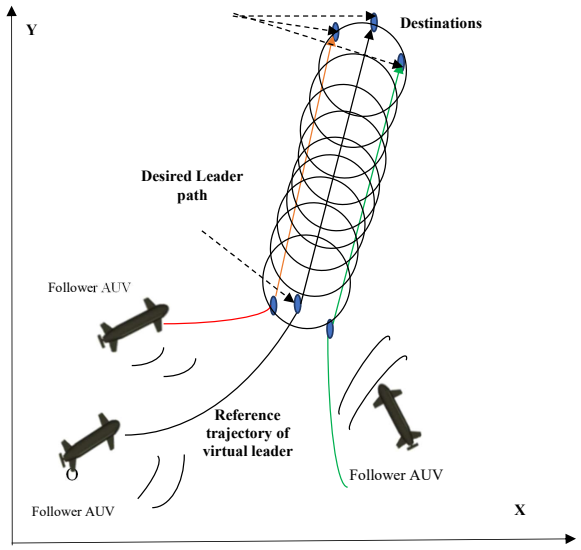

***Fig. 1**: Path planning using bio-inspired MAS.*

yaw quadratic drag coefficients, respectively, which are also taken as model parameters. The control input is represented as T.

This paper aims to solve the path planning problem using bio-inspired MAS where each agent reaches their desired destination using the position estimation technique. The MAS represents a system of identical AUVs deployed for the mission. The AUVs travel from different starting points to different predefined destinations while maintaining a coordinated shape. The proposed MAS controller is designed to obtain a stable shape and plan the path of agents to reach their destination using the position estimation technique. The agents switch from one state to another and progress over time until the desired shape is obtained. The DPC algorithm is proposed to implement a distance constraint that maintains a safe distance among neighboring AUVs and helps in avoiding collision among them. The path cost is optimized using the distance constraint for each AUV position along the path. Once the desired coordinated shape is obtained, it is maintained by the agent AUVs while approaching their destination, as shown in Fig. 1.

The DPC algorithm is applied separately to the path of each agent to obtain an optimum position for maintaining the coordinated shape. At the optimized position, the agent AUVs are at a safe distance from the neighbor AUVs without loss of communication among them. Its aim is to find K paths for K agent AUVs with the optimized path cost defined as $\hat{P}_k$ for $(1 < k < K)$ through the defined directed graph $\mathcal{G}_k$ such that

$$\left\{\hat{P}_1, \ldots, \hat{P}_K\right\} = \underset{\hat{P}_1,\ldots,\hat{P}_K}{\operatorname{argmin}} \sum_{k=1,\ldots,K} c_{\mathcal{E}}\left(\hat{P}_k\right) \tag{5}$$

Eq. (4) is subject to the distance constraint given by

$$d\left(\hat{P}_k(t), \hat{P}_l(t)\right) \leq \pi_{kl}(t) \;\; \forall \;\; (1 \leq t \leq \tau) \tag{6}$$

where $1 \leq k \leq K$, $1 \leq l, k \leq K$, and $k \neq l$.

The goal of an optimal planning algorithm is to find K paths π_{kl} through the corresponding graph. The environment is modeled as a 2D grid map, assuming that all the AUVs are on the same depth. Since the environment is free from obstacles, the AUVs need only to avoid collision among themselves.

3. COMMUNICATION CONSENSUS

In a directed graph $\mathcal{G}_k = (N, \mathcal{E}, A)$, while $k = \{1, 2, \ldots, K\}$ with N set of nodes and $\mathcal{E} \subseteq (N \times N)$ set of edges can be used to represent the interaction topology of K agent AUVs connected through a communication network. Here, A represents a vector of non-negative values such that $A = \left[a_{kl}\right] \in R^{|\mathcal{E}|\times|\mathcal{E}|}$ and $|\mathcal{E}|$ is the cardinality of $\mathcal{E}$. The positive a_{kl} gives the binary value for k^{th} and l^{th} AUVs are immediate neighbors with a communication edge, otherwise the $a_{kl} = 0$. The degree of the k^{th} node is given by $d_k = \sum_{l\in K} a_{kl}$. The Δ is the degree matrix of $\mathcal{G}_k$, which is a $(K \times K)$ diagonal matrix of d_k. The positive semi-definite Laplacian matrix of $\mathcal{G}_k$ is defined by $L = \Delta - A = \left[\ell_{kl}\right]$, where ℓ_{kl} is

$$\ell_{kl} = \begin{cases} \sum\limits_{l\in K_k} a_{kl}; & \forall \;\; k = l \\ -a_{kl}; & \forall \;\; k \neq l. \end{cases} \tag{7}$$

The $\mathcal{G}_k$ is formed by 'i' subspaces where $1 < i < K$. The target-driven path planning of any k^{th} agent AUV_k in a MAS can be described as finding a path with the minimum path cost through $\mathcal{G}_k$. A time index can be added as an additional variable to $\mathcal{G}_k$ such that $\mathcal{G}_{tk} = \mathcal{G}_k \times \{0, 1, 2, \ldots, \tau\}$ to obtain a time parametrized path [8]. Each node represents a state $\{s, t\}$ given by the position coordinates of an agent AUV $\{x, y\}$ such that $s \in N\left(\mathcal{G}_{tk}\right)$ at a time instant t. An agent AUV can only move from one state s to the next free state $\hat{s}$ along the edge represented by $\{s, t\} \rightarrow \{\hat{s}, t+1\} \in \mathcal{E}\left(\mathcal{G}_{tk}\right)$, such that $\hat{s} \in \mathcal{E}\left(\mathcal{G}_k\right)$ or $s \rightarrow \hat{s} \in \mathcal{E}\left(\mathcal{G}_k\right)$. This condition guarantees only the forward movement of AUVs over time. Each edge is associated with a positive cost factor $c_{\mathcal{E}}(s, \hat{s})$. The cost is represented by the Euclidian distances between the neighboring cell centers. Each path from the start to the destination point is assumed to be accomplished in τ–time steps. Thus, the path of k^{th} AUV can be given as $P_k = \left\{\text{start}_k, s_1, \ldots, \text{target}_k\right\}$. The path cost of path P_k can be defined as

$$c_{\mathcal{E}}\left(P_k\right) = \sum_{i=1,\ldots,\tau} c_{\mathcal{E}}\left(s_{i-1}, s_i\right). \tag{8}$$

The maximum Euclidian distance between a pair of neighbor AUVs is considered without breaking communication between them as a constraint π_{kl} for all $k \neq l$. The distance between k^{th} and l^{th} AUVs is defined as $d(s, \hat{s})$ representing a positive scalar quantity for any pair of states such that $s \in N\left(\mathcal{G}_k\right)$, $\hat{s} \in N\left(\mathcal{G}_l\right)$ for $k \neq l$. Hence, $\pi_{kl}(t)$ can be defined as a vector consisting of τ

positive distance values $d(\cdot,\cdot)$ between k^{th} and l^{th} AUVs at time instant t.

The coordination among AUVs results in a rendezvous in space [11] consensus problem, where K agent AUVs reach a consensus with an interactive switching topology through position estimation. In real-world conditions, it is difficult to find the exact position η_k of the k^{th} agent AUV. So the following assumptions are made according to [26]:

i. Each k^{th} agent AUV estimates the relative position of the neighboring l^{th} AUV since it is unable to obtain the exact position. Thus, the relative position of l^{th} AUV to k^{th} AUV can be calculated as

$$\eta_{lk} = \eta_l - \eta_k \quad \forall \quad (1 \le k \le K), \tag{9}$$

where $1 \le l \le K$, $k \ne l$.

ii. Each AUV can measure its own actual velocity and also obtain the information velocity of its neighbor through the communication network.

iii. The k^{th} agent AUV can estimate its own position as $\hat{\eta}_k$ for $k = 1, \ldots, K$ and also obtain the position estimation of its neighbor AUV within its communication range, defined by the distance constraint $\pi_{ij}(t)$.

iv. The environment is free of static obstacles. Thus, the AUVs act as dynamic obstacles and avoid collision among themselves by position estimation.

Now the desired position of an agent AUV in the interactive graph $\mathcal{G}_k$ can be defined as η_{kd} where, $k = \{1, 2, \ldots, K\}$.

Lemma 1: For any number

$$\sigma = \frac{\gamma\mu - \beta \pm \sqrt{(\gamma h - \beta)^2 + 4\mu}}{2}$$

where $\sigma,\ \mu \in \mathbb{C}$. If $\beta \ge 0$, $\mathrm{Re}(\mu) < 0$, $\mathrm{Im}(\mu) > 0$, and

$$\zeta(\mu) = \sqrt{\frac{2}{|\mu| \cos\left[\tan^{-1}\frac{\mathrm{Im}(\mu)}{-\mathrm{Re}(\mu)}\right]}},$$

then Re < 0. Here, Re$(\cdot)$ and Im$(\cdot)$ are the real and imaginary parts of a number respectively. σ, γ and β are a non-negative constant. For such condition

$$\gamma > \zeta(\mu) \tag{10}$$

Lemma 2: For the system given by Eq. (1) a control law T_{kl} as given in [7] can be used, such that

$$T_k = \sum_{l=1}^{K} a_{kl}(t)\left[\left(\eta_k - \eta_l\right) + \gamma\left(V_k - V_l\right)\right]. \tag{11}$$

The MAS of AUVs obtains consensus asymptotically if and only if $\partial = \begin{bmatrix} 0_{K\times K} & I_K \\ -L_K(t) & \gamma L_K(t) \end{bmatrix}$ has two eigen values equal to "0", and the rest have negative real parts. Here, $\eta_k(t) \to \sum_{k=1}^{K} \eta_k \eta_k(0) + \sum_{k=1}^{K} \eta_k V_k(0)$ and $V_k(t) \to \sum_{k=1}^{K} \eta_k V_k(0)$ for larger value of t, where $\eta = \left[\eta_1, \ldots, \eta_k\right]^T \ge 0$, ${I_K}^T \eta = 1$, ${L_K}^T \eta = 0$.

Lemma 3: Assuming that the directed graph $\mathcal{G}_k$ has a spanning tree and the Laplacian matrix given by L, $\eta_k = \{\eta_1, \eta_2, \ldots, \eta_K\} \in R^K$ of the linear system given in Eq. (5) exponentially converges to a finite vector $\eta_k^{\infty} = \{\eta_c^{\infty}, \ldots, \eta_c^{\infty}\} \in R^K$ [7].

The formation controller for the multi-AUV system is designed to achieve the following objectives:

i. To design an estimation law for a k^{th} agent AUV that satisfies

$$\lim_{t\to\infty} \hat{\eta}_k(t) = \eta_k(t) + \widetilde{\eta_k^{\infty}} \tag{12}$$

where, the $\hat{\eta}_k$ estimated position of the agent AUV, $\eta_k^{\infty} \in R^k$ represents a constant vector using η_{kl} and $\hat{\eta}_l \ \forall\ l \in K_k$. As presented in Eq. (12), the estimated position $\hat{\eta}_k$, instead of converging into η_k converges into $\eta_k + \widetilde{\eta_k^{\infty}}$.

ii. To formulate the optimal control law for a set of desired positions of AUV $\eta_{kd}, k \in N$ as per the designed estimator such that all the agent AUVs reach their respective desired positions with a constant error given by,

$$\begin{aligned} &\lim_{t\to\infty} \hat{\eta}_k(t) = \eta_{kd}(t) + \widetilde{\eta_k^{\infty}} \ \text{ and} \\ &\lim_{t\to\infty} V_k(t) = 0 \end{aligned} \tag{13}$$

for $k \in \{1, 2, \ldots, K\}$, where $\eta_k^{\infty} \in R^K$ is a constant vector and η_{kd} is the desired input. The energy cost is defined by the quadratic performance index [7] as follows:

$$\mathbb{J} = \frac{1}{2}\sum_{k=1}^{K}\left\{\int_0^{\infty}\left[e_k(t)^T Q e_k(t) + T_k^T F T_k\right] dt\right\}. \tag{14}$$

Here, $e_k(t) = \eta_{kd}(t) - \hat{\eta}_k(t)$ gives the error in output, Q and F are assumed to be positive definite matrices of the required dimensions. As per Eq. (13), the estimated position $\hat{\eta}_k$, instead of converging to desired position η_{kd} converges to $\eta_{kd} + \widetilde{\eta_k^{\infty}}$, because of the constant error $e_k(t)$.

iii. To propose a consensus law as per the designed estimator for a set of agent AUVs so as to make them converge into a consistent value of position and velocity, such that

$$\begin{aligned} &\lim_{t\to\infty} \eta_k(t) = \lim_{t\to\infty} \eta_l(t) \ \text{ and} \\ &\lim_{t\to\infty} V_k(t) = \lim_{t\to\infty} V_l(t) = \text{constant} \end{aligned} \tag{15}$$

for all $k, l \in \{1, 2, \ldots, K\}$.

The final velocities of all the agents presented in Eq. (14) converge into a constant value determined by the initial velocities of all the agent AUVs.

In this paper, the available data is obtained only through the communication network. The relative

position of k^{th} and l^{th} neighbor AUVs (η_{kl}) estimated positions of a pair of neighbor AUVs $(\hat{\eta}_k, \hat{\eta}_l)$, and velocity measurement V_k are calculated based on the information received.

4. CONTROLLER DESIGN

4.1 Proposed Position Estimator

For agent AUVs with dynamics, a distributed estimation law [26] can be designed as follows:

$$\begin{aligned}\dot{\hat{\eta}}_k &= v_k + \mathbb{i}_0 \sum_{l=1}^{K} a_{kl}\left(\hat{\eta}_{lk} - \eta_{lk}\right) \\ &= \dot{\eta_k} + \mathbb{i}_0 \sum_{l=1}^{K} a_{kl}\left[\left(\hat{\eta}_l - \hat{\eta}_k\right) - \left(\eta_l - \eta_k\right)\right] \end{aligned} \tag{16}$$

where $\mathbb{i}_0$ is a positive real number, the estimation of relative position of l^{th} and k^{th} AUV is $\hat{\eta}_{lk}$. The required velocity v_k is calculated. The information on the relative position (η_{lk}) and estimation of position l^{th} for the AUV $(\hat{\eta}_l)$ can be obtained through the communication network. If $\tilde{\eta}_k = \eta_k - \hat{\eta}_k$, then Eq. (16) can be rewritten as follows:

$$\dot{\tilde{\eta}}_k = \mathbb{i}_0 \sum_{l=1}^{K} a_{kl}\left(\tilde{\eta}_l - \tilde{\eta}_k\right). \tag{17}$$

Thus, the error dynamics of the overall MAS can be estimated as the Kronecker product of Laplacian matrix L and identity matrix I $(L \otimes I)$ such that;

$$\dot{\tilde{\eta}} = -\mathbb{i}_0 (L \otimes I)\,\tilde{\eta} \tag{18}$$

where $\tilde{\eta} = \left\{\tilde{\eta}_1, \ldots, \tilde{\eta}_K\right\}$.

Lemma 4: Assuming that the directed graph $\mathcal{G}_k$ has a spanning tree, the estimation of error dynamics $\hat{\eta}_k$ can globally exponentially converge to $\tilde{\eta} - \tilde{\eta}_k^{\infty}$, where $\tilde{\eta}_k^{\infty} = \left\{\eta_c^{\infty}, \ldots, \eta_c^{\infty}\right\}$ is a finite vector $\eta_k^{\infty} = \left\{\eta_c^{\infty}, \ldots, \eta_c^{\infty}\right\}$ [26].

Lemma 5: Let $\lambda_2, \ldots, \lambda_{D+1} \neq 0$ be the D distinct nonzero eigenvalues of the graph Laplacian matrix L, then, up to permutation, the sequence $\left\{\alpha_i\right\}_{i=1,\ldots,D}$ with $\alpha_i = 1/\lambda_{i+1}$, $i = 1, 2, \ldots, D$, is the unique sequence allowing the minimal factorization of the average consensus matrix to be obtained as

$$\frac{1}{N} 1 1^T = \prod_{i=1}^{D} \left(\mathrm{I}_N - \alpha_i L\right). \tag{19}$$

Proof: Let us consider the following factorization of the average consensus matrix:

$$\frac{1}{N} 1 1^T = \prod_{i=1}^{\theta=1} \left(\mathrm{I}_N - \alpha_i L\right). \tag{20}$$

The Laplacian matrix L being symmetric, then: $L = U \Delta U^T$, $U^T U = I_N$, $U U^T = I_N$ where $\Delta = \operatorname{diag}\left(\lambda_1, \lambda_2, \ldots, \lambda_N\right)$ and $U = \left(1/\sqrt{N}\right) 1 \widetilde{U}$ with $\widetilde{U}^T \widetilde{U} = I_{N-1}$ and $\widetilde{U}^T 1 = 0$. Therefore, the above factorization can be written as:

$$U \left(\prod_{i=1}^{\theta=1} \left(\mathrm{I}_N - \alpha_i \Delta\right) \right) U^T = \frac{1}{N} 1 1^T, \tag{21}$$

or equivalently:

$$U \left(\prod_{i=1}^{\theta=1} \left(\mathrm{I}_N - \alpha_i \Delta\right) \right) U^T = U \operatorname{diag}(10, \ldots, 0)\, U^T. \tag{22}$$

From Eq. (22), it can be observed that $\prod_{i=1}^{\theta=1} \left(1 - \alpha_i \lambda_1\right) = 1$, is always fulfilled since $\lambda_1 = 0$. In addition, we have:

$$\prod_{i=1}^{\theta=1} \left(1 - \alpha_i \lambda_j\right) = 0, \quad j = 2, \ldots, N. \tag{23}$$

Taking into account the multiplicities of the eigen values, D distinct equations are available. D equalities are fulfilled only if $1 / \alpha_i$ belong to the Laplacian spectrum and at least D distinct α_i exist. Therefore, the Laplacian spectrum implies the minimal factorization of the average consensus matrix. ■

4.2 Derivation of Control Input Based on Consensus Law

According to the aforementioned assumption and position estimator design, the feedback control law for the MAS of AUVs can be defined as:

$$T_k = \sum_{l=1}^{K} a_{kl}\left[\left(\hat{\eta}_k - \eta_{kd}\right) - \left(\hat{\eta}_l - \eta_{ld}\right) + \gamma\left(v_k - v_l\right)\right]. \tag{24}$$

Using Eq. (24), the desired formation of MAS may be obtained if $\hat{\eta}_k \to \eta_{kd}$ and $\hat{\eta}_l \to \eta_{ld}$ for all $k, l \in \{1, 2, \ldots, K\}$ as $\left\|\hat{\eta}_k - \eta_{kd}\right\| - \left\|\hat{\eta}_l - \eta_{ld}\right\| \to 0$ and $\left\|v_k - vl\right\| \to 0$.

When converging into a desired position the agent AUVs should not collide with each other. Thus, a distance constraint should be incorporated into the formation controller. Implementation of the distance constraint needs a controller design with extra control terms. The potential function is designed according to the position estimator as follows:

$$\mathbb{V}_{kl}\left(\hat{\eta}_k, \hat{\eta}_l\right) = \left(\min\left\{ 0, \frac{\left\|\hat{\eta}_k - \hat{\eta}_l\right\|^2 - \Re^2}{\left\|\hat{\eta}_k - \hat{\eta}_l\right\|^2 - \mathbb{r}^2} \right\} \right)^2. \tag{25}$$

$$\frac{\partial \mathbb{V}_{kl}^{T}}{\partial \hat{\eta}_k} = \begin{cases} \dfrac{4\left(\mathfrak{R}^2 - \mathbb{r}^2\right)\left(\left\|\hat{\eta}_k - \hat{\eta}_l\right\|^2 - \mathfrak{R}^2\right)}{\left(\left\|\hat{\eta}_k - \hat{\eta}_l\right\|^2 - \mathbb{r}^2\right)^3}\left(\hat{\eta}_k - \hat{\eta}_l\right)^T \\ 0 \end{cases} \tag{26}$$

$$T_k^a = -\sum_{l=1}^{K} a_{kl}\left[\left(\left(\hat{\eta}_k - \eta_{kd}\right) - \left(\hat{\eta}_l - \eta_{ld}\right)\right) + \gamma\left(v_k - v_l\right)\right] - \sum_{l=1}^{K} \frac{\partial \mathbb{V}_{kl}\left(\hat{\eta}_k, \hat{\eta}_l\right)^T}{\partial \hat{\eta}_k} \tag{27}$$

Here $\mathfrak{R}$ and $\mathbb{r}$ define the detection radius of the AUV and the safest distance for avoiding inter-vehicle collision, respectively. If the inter-vehicle distance between agent AUVs is less than $\mathfrak{R}$, then $\mathbb{V}_{kl}\left(\hat{\eta}_k, \hat{\eta}_l\right)$ is positive and will be included in the additional control input. By finding the partial derivative of Eq. (25) with respect to $\hat{\eta}_k$, we can get Eq. (26).

Now the control law for formation control with collision avoidance based on position estimation can be defined using Eqs. (24) and (26) as Eq. (27).

Theorem 1: As presented in Eqs. (11) and (27), the given MAS may obtain the desired formation if the directed graph $\mathcal{G}_k$ has a spanning tree, and if

$$\gamma > \overline{\gamma} \tag{28}$$

where $\gamma \triangleq 0$ if all the $(K-1)$ nonzero eigen values of $-L_n$, given by $\mu_k \ \forall\ k \in \{1, \ldots, K\}$ are negative and $\overline{\gamma}_{\max \mu_k, \forall k \in \{1,\ldots,K\}} \zeta\left(\mu_k\right)$. Therefore, for $t \to \infty$, we have $\eta_k(t) \to \eta_{kd} + \tilde{\eta}_c^{\infty} + t\sum_{k=1}^{K} \eta_k v_k(0)$ and $v_k(t) \to \sum_{k=1}^{K} \eta_k v_k(0)$ where $\eta = \left[\eta_1, \ldots, \eta_k\right]^T \geq 0$, ${I_K}^T \eta = 1$, ${L_K}^T \eta_k = 1$, $\tilde{\eta}_k^{\infty} = \left\{\tilde{\eta}_c^{\infty}, \ldots, \tilde{\eta}_c^{\infty}\right\}$, $\eta_{kd} = \left\{\eta_{1d}, \eta_{2d}, \ldots, \eta_{Kd}\right\}$ are constants [25].

Theorem 2: If the controller is designed as presented in Eq. (27) for the system described in Eq. (1) and γ satisfies Eq. (28), then the multi-AUV system obtains its desired formation without inter-vehicular collision [26]. The proof of Theorems 1 and 2 is referred to in [26].

4.3 Distributed Path Consensus (DPC) Algorithm

The DPC algorithm is used in this research for planning a safe path for the AUVs to reach the desired destination by applying the distance constraint in a 2D underwater environment. Path planning is separately incorporated for each agent using DPC to find K optimal safe paths for K agent AUVs defined as $\widehat{P}_k$ for $(1 < k < K)$ through the defined directed graph $\mathcal{G}_k$, as shown in Eq. (5) subject to the constraints defined in Eq. (6). For every iteration (*iter*), the DPC algorithm searches for a subset of graph $\mathcal{G}_{sub}$ to find the optimized cost path for an agent AUV [22, 23]. The path cost represents the summation of the distance traveled by an AUV and the penalty imposed due to the violation of distance constraints. The penalty for violation increases with each iteration by slowly increasing the weights associated with the cross points. The cross points are those on the planned path where two paths may collide with each other. Thus, the path cost of generated paths going through the cross points increases due to the violation of distance constraints. Hence, these paths are avoided while planning the optimized path. The penalty function $\lambda_{kl}\left(\widehat{P}_k, \widehat{P}_l, \pi_{kl}\right)$, $k \neq l$ used for constraint violation is given by

$$\lambda_{kl}\left(\widehat{P}_k, \widehat{P}_l, \pi_{kl}\right) \sum_{t=1,2,\ldots,\tau} \widetilde{\omega}_{kl}\left(\widehat{P}_k(t), \widehat{P}_l(t), \pi_{kl}(t)\right). \tag{29}$$

If ω_{kl} is the dynamic weight associated with the edge $s \to \hat{s} \in \mathcal{E}\left(\mathcal{G}_k\right)$ such that $\omega_{kl} = \omega_{lk}$ then $\widetilde{\omega}_{kl}$ can be defined as

$$\omega_{kl}\left(s, \hat{s}, \pi_{kl}\right) = \max\left(0, d\left(s, \hat{s}\right) - \pi_{kl}\right). \tag{30}$$

As π_{kl} is a constant for the research problem in this study, it can be dropped. Hence, $\lambda_{kl}\left(\widehat{P}_k, \widehat{P}_l, \pi_{kl}\right)$ is represented as $\lambda\left(\widehat{P}_k, \widehat{P}_l\right)$. The association of ω_{kl} with π_{kl} is used to convert the hard distance constraint defined in Eq. (6) into a soft distance constraint [23]. The path cost is computed by calculating the Euclidian distance between the AUVs using position estimation. The DPC algorithm is then used iteratively on each agent AUV to optimize the cost. For the k^{th} agent AUV, the weight of penalty increases by a small amount $\mho_{kl}^{i}$ with each iteration. The value of $\mho_{kl}^{i}$ is calculated as

$$\mho_{kl}^{i} \begin{cases} \geq 0, & \forall\ k \neq l \\ = 0, & \text{otherwise.} \end{cases} \tag{31}$$

Thus, the minimum cost path computed for k^{th} AUV can be given as $P_k = \left\{\text{start}_k, s_1, \ldots, \text{target}_k\right\}$ in $\mathcal{G}_{tk}$. The cost associated with the transition $\{s, t\} \to \{\hat{s}, t+1\} \in \mathcal{E}\left(\mathcal{G}_{tk}\right)$ has been modified using

$$c_{\mathcal{E}}(s, \hat{s})\, 2 \sum_{l=1,\ldots,K, \forall\, k \neq l} {\omega_{kl}}^{iter+1} \lambda_{kl}\left(\hat{s}, \widehat{P}_l^{iter}(t), \pi_{kl}(t)\right). \tag{32}$$

For each iteration *iter* and i^{th}, AUV path can be calculated as Eq. (33). The flow chart of the DPC algorithm used for path planning is presented in Fig. 2.

Lemma 6: As the graph is directed [8], $\mathcal{G}_k$ contains a spanning tree with the leader as the root node, i.e.,

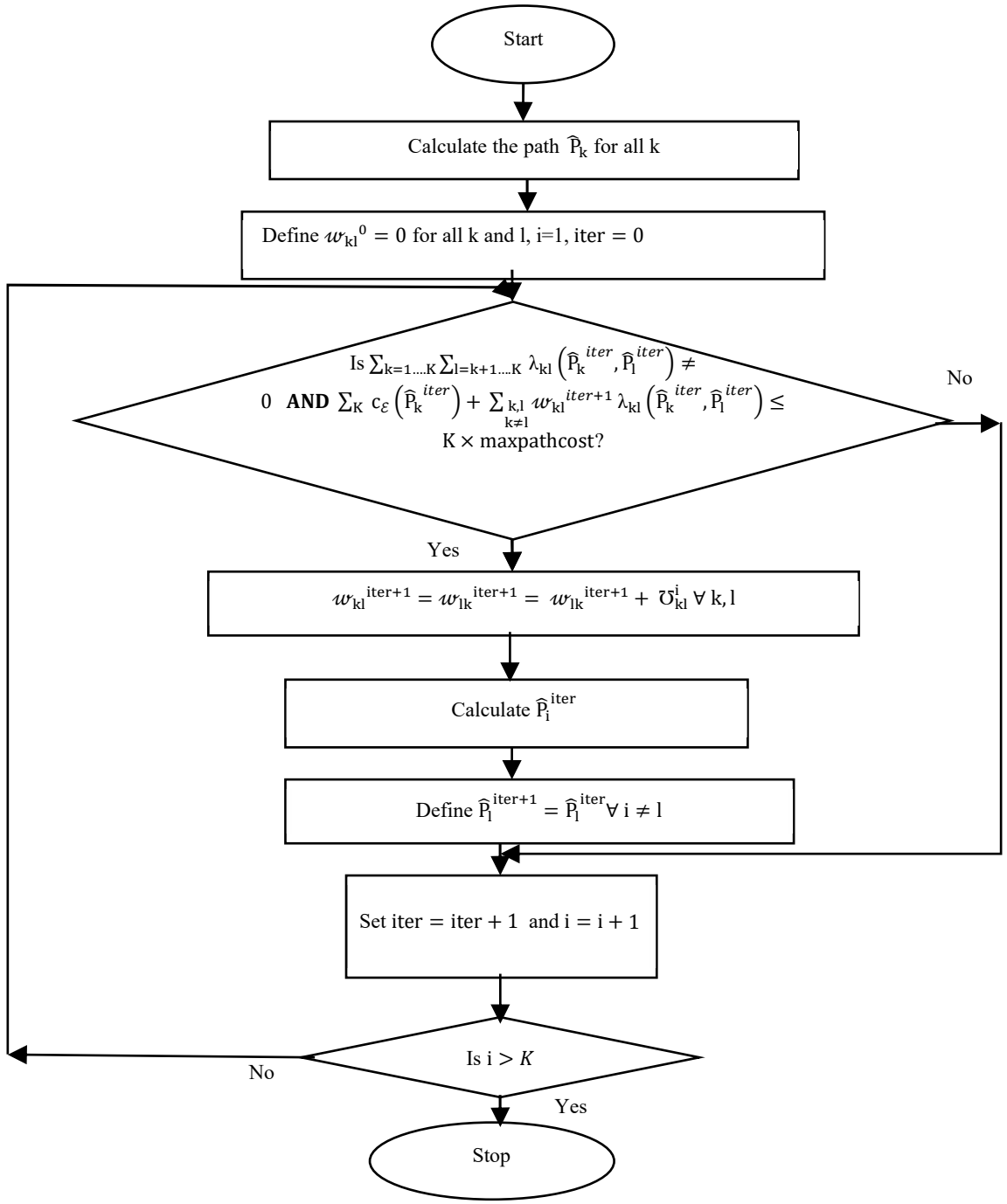

***Fig. 2**: Flow chart of the DPC algorithm.*

$B \neq 0$, then $H = L + B$ is of full rank. Furthermore, $\left[p_1, p_2, \ldots, p_N\right]^T = H^{-T}1_N$. Thus, Eq. (34).

The diagonal matrix P and symmetric matrix Q are then both positively defined. Observing $\hat{z}_i = -H^{-T}\widehat{P}_i$, the convergence of $\widehat{P}_i$ follows on from the convergence of $\hat{z}_i$ provided that certain conditions are satisfied. Let an induction analysis for $\gamma > 1$ be used for the convenience of presentation, and the Lyapunov candidate function may then be derived as Eq. (35). Then, we have Eq. (36), where $\overline{p} \underline{\Delta} \max\left\{p_1, p_2, \ldots, p_N\right\}$ and $Q = \left(PH + H^T P\right)/2$ is invoked. Let $\alpha_n \underline{\Delta} b_n \overline{u}_0 \overline{p}/\lambda_{\min}^Q$ and for $\gamma > 1$, V_n verifies as Eq. (37).

Case i) For $\sum_{i=1}^N \left|z_n^i\right| > 1$, from Eq. (16) we have

$$V_n \leq \alpha_n \overline{p} \sum_{i=1}^N \left|z_n^i\right| + \frac{\beta_n \overline{p}}{1+\gamma}\left(\sum_{i=1}^N \left|z_n^i\right|\right)^{1+\gamma}$$

$$\leq \overline{p}\left(\alpha_n + \frac{\beta_n \overline{p}}{1+\gamma}\right)\left(\sum_{i=1}^N \left|z_n^i\right|\right)^{1+\gamma}.$$

$$\begin{aligned}\widehat{P}_i^{iter} &= \underset{P_i}{\operatorname{argmin}} \left\{ c_{\mathcal{E}}\left(\widehat{P}_i\right) + \sum_{k=1,\ldots,K,\ k\neq i} {\omega_{ki}}^{iter+1} \lambda_{ki}\left(\widehat{P}_k^{iter}, \widehat{P}_i\right) + \sum_{l=1,\ldots,K,\ l\neq i} {\omega_{li}}^{iter+1} \lambda_{li}\left(\widehat{P}_i, \widehat{P}_l^{iter}\right) \right\} \\ &= \underset{P_i}{\operatorname{argmin}} \left\{ c_{\mathcal{E}}\left(\widehat{P}_i\right) + 2 \sum_{l=1,\ldots,K,\ k\neq i} {\omega_{ki}}^{iter+1} \lambda_{ki}\left(\widehat{P}_k^{iter}, \widehat{P}_i\right) \right\} \end{aligned} \tag{33}$$

$$P = \operatorname{diag}\left\{p_1, p_2, \ldots, p_N\right\} \quad \text{and} \quad Q = \frac{PH + H^T P}{2} \tag{34}$$

$$V_n = \sum_{i=1}^{N} p_i \left(\alpha_n \left| z_n^i \right| + \frac{\beta_n}{1+\gamma} \left| z_n^i \right|^{1+\gamma} \right) \tag{35}$$

$$\begin{aligned}\dot{V}_n &= \sum_{i=1}^{N} p_i \left(\alpha_n \operatorname{sign}\left(z_n^i\right) + \beta_n \left[z_n^i\right]^{\gamma} \right) \\ &\quad \times \left[\alpha_n \left(\sum_{j=1}^{N} a_{ij} \left(\operatorname{sign}\left(z_n^j\right) - \operatorname{sign}\left(z_n^i\right) \right) - b_i \operatorname{sign}\left(z_n^i\right) \right) + \beta_n \left(\sum_{j=1}^{N} a_{ij} \left(\left[z_n^j\right]^{\gamma} - \left[z_n^i\right]^{\gamma} \right) - b_i \left[z_n^j\right]^{\gamma} \right) - b_n u_0 \right] \\ &= -\left(\alpha_n \operatorname{sign}\left(z_n\right) + \beta_n \left[z_n\right]^{\gamma} \right)^T PH \left(\alpha_n \operatorname{sign}\left(z_n\right) + \beta_n \left[z_n\right]^{\gamma} \right) - \sum_{i=1}^{N} p_i \left(\alpha_n \operatorname{sign}\left(z_n^i\right) + \beta_n \left[z_n^i\right]^{\gamma} \right) b_n u_0 \\ &= -\left(\alpha_n \operatorname{sign}\left(z_n\right) + \beta_n \left[z_n\right]^{\gamma} \right)^T Q \left(\alpha_n \operatorname{sign}\left(z_n\right) + \beta_n \left[z_n\right]^{\gamma} \right) - \sum_{i=1}^{N} p_i \left(\alpha_n \operatorname{sign}\left(z_n^i\right) + \beta_n \left[z_n^i\right]^{\gamma} \right) b_n u_0 \\ &\leq -\lambda_{\min}^{Q} \sum_{i=1}^{N} \left(\alpha_n^2 + 2\alpha_n \beta_n \left| z_n^i \right|^{\gamma} + \beta_n^2 \left| z_n^i \right|^{2\gamma} \right) + \alpha_n b_n \bar{u}_0 N \bar{p} + \beta_n b_n \bar{u}_0 \bar{p} \sum_{i=1}^{N} \left[z_n^i\right]^{\gamma} \end{aligned} \tag{36}$$

$$\dot{V}_n \leq -\lambda_{\min}^{Q} \beta_n \sum_{i=1}^{N} \left(\alpha_n \left| z_n^i \right|^{\gamma} + \beta_n \left| z_n^i \right|^{2\gamma} \right) \leq -\lambda_{\min}^{Q} \alpha_n \beta_n N^{1-\gamma} \left(\sum_{i=1}^{N} \left| z_n^i \right| \right)^{\gamma} - \lambda_{\min}^{Q} \beta_n^2 N^{1-2\gamma} \left(\sum_{i=1}^{N} \left| z_n^i \right| \right)^{2\gamma} \tag{37}$$

$$\sum_{i=1}^{N} \left| z_n^i \right| \geq \left(\frac{V_n}{\bar{p}\left(\alpha_n + \frac{\beta_n}{1+\gamma} \right)} \right)^{\frac{1}{1+\gamma}} \tag{38}$$

Then, we have Eq. (38). Substituting Eq. (37) into Eq. (36) yields Eq. (39).

Case ii) For $\sum_{i=1}^{N} \left| z_n^i \right| < 1$, from Eq. (36) we have

$$V_n \leq \bar{p} \left(\alpha_n + \frac{\beta_n}{1+\gamma} \right) \sum_{i=1}^{N} \left| z_n^i \right| \quad \text{and}$$

$$\sum_{i=1}^{N} \left| z_n^i \right| \geq \left(\frac{V_n}{\bar{p}\left(\alpha_n + \frac{\beta_n}{1+\gamma} \right)} \right).$$

Substituting Eq. (39) into Eq. (36) obtains Eq. (40).

Considering the following Lyapunov function candidate for k steps, we have Eq. (41), where $k = 1, 2, \ldots, N-1$. Differentiating Eq. (15) along Eq. (8) obtains Eq. (42), where $H = L + B$ and $Q = (PH + H^T P)/2$ are used to derive the second equality. If $\sum_{i=1}^{N} \left| z_{k+1}^i \right| \leq 1$ holds, then we have

$$\begin{aligned}\dot{V}_k &\leq -\lambda_{min}^{Q} \sum_{i=1}^{N} \left(\alpha_k^2 + 2\alpha_k \beta_k \left| z_k^i \right|^{\gamma} + \beta_k^2 \left| z_k^i \right|^{2\gamma} \right) \\ &\quad + \alpha k \bar{p} N + \beta k \bar{p} \sum_{i=1}^{N} \left| z_k^i \right|^{\gamma}. \end{aligned}$$

$$\dot{V}_n \leq -\frac{\lambda_{\min}^{Q}\alpha_n\beta_n N^{1-\gamma}}{\overline{p}^{\frac{1}{1+\gamma}}\left(\alpha_n+\frac{\beta_n}{1+\gamma}\right)^{\frac{1}{1+\gamma}}}V_n^{\frac{\gamma}{1+\gamma}}-\frac{\lambda_{\min}^{Q}\alpha_n\beta_n^2 N^{1-2\gamma}}{\overline{p}^{\frac{1}{1+\gamma}}\left(\alpha_n+\frac{\beta_n}{1+\gamma}\right)^{\frac{1}{1+\gamma}}}V_n^{\frac{2\gamma}{1+\gamma}} \tag{39}$$

$$\dot{V}_n \leq -\frac{\lambda_{\min}^{Q}\alpha_n\beta_n N^{1-\gamma}}{\overline{p}\left(\alpha_n+\frac{\beta_n}{1+\gamma}\right)}V_n^{\gamma}-\frac{\lambda_{\min}^{Q}\alpha_n\beta_n^2 N^{1-2\gamma}}{\overline{p}\left(\alpha_n+\frac{\beta_n}{1+\gamma}\right)}V_n^{2\gamma} \tag{40}$$

$$V_k=\sum_{i=1}^{N}p_i\left(\alpha_k\left|z_k^i\right|+\frac{\beta_k}{1+\gamma}\left|z_k^i\right|^{1+\gamma}\right) \tag{41}$$

$$\begin{aligned}\dot{V}_k &= \sum_{i=1}^{N}p_i\left(\alpha_k\mathrm{sign}\left(z_k^i\right)+\beta_k\left[z_k^i\right]^{\gamma}\right)\left(z_{k+1}^i+\alpha_k\left(\sum_{j=1}^{N}\alpha_{ij}\left(\mathrm{sign}\left(z_k^j\right)-\mathrm{sign}\left(z_k^i\right)\right)-b_k\mathrm{sign}\left(z_k^i\right)\right)\right.\\ &\qquad\left.+\beta_k\left(\sum_{j=1}^{N}\alpha_{ij}\left(\left[z_k^j\right]^{\gamma}-\left[z_k^i\right]^{\gamma}\right)-b_k\left[z_k^j\right]^{\gamma}\right)\right)\\ &= -\left(\alpha_k\mathrm{sign}\left(z_k\right)+\beta_k\left[z_k\right]^{\gamma}\right)^{T}Q\left(\alpha_k\mathrm{sign}\left(z_k\right)+\beta_k\left[z_k\right]^{\gamma}\right)+\sum_{i=1}^{N}p_i\left(\alpha_k\mathrm{sign}\left(z_k^i\right)+\beta_k\left[z_k^i\right]^{\gamma}\right)z_{k+1}^i\\ &\leq -\lambda_{\min}^{Q}\sum_{i=1}^{N}\left(\alpha_k^2+2\alpha_k\beta_k\left|z_k^i\right|^{\gamma}+\beta_k^2\left|z_k^i\right|^{2\gamma}\right)+\alpha_k\sum_{i=1}^{N}p_i\left|z_{k+1}^i\right|+\beta_k\sum_{i=1}^{N}p_i\left|z_k^i\right|^{\gamma}\left|z_{k+1}^i\right|\end{aligned} \tag{42}$$

$$\begin{aligned}\dot{V}_k &\leq -\lambda_{\min}^{Q}\beta_k\sum_{i=1}^{N}\left(\alpha_k\left|z_k^i\right|^{\gamma}+\beta_k\left|z_k^i\right|^{2\gamma}\right)\\ &\leq -\lambda_{\min}^{Q}\alpha_k\beta_k N^{1-\gamma}\left(\sum_{i=1}^{N}\left|z_k^i\right|\right)^{\gamma}-\lambda_{\min}^{Q}\beta_k^2 N^{1-2\gamma}\left(\sum_{i=1}^{N}\left|z_k^i\right|\right)^{2\gamma}\end{aligned} \tag{43}$$

Let $\alpha_k\underline{\Delta}\overline{p}/\lambda_{\min}^{Q}$ and for $\gamma>1$, $\dot{V}_k$ verifies as Eq. (43).

Likewise, the following two cases are considered:
Case iii) For $\sum_{i=1}^{N}\left|z_k^i\right|\geq 1$, it follows Eq. (41) that

$$\sum_{i=1}^{N}\left|z_k^i\right|\geq\left(\frac{V_k}{\tilde{p}\left(\alpha_k+\frac{\beta_k}{1+\gamma}\right)}\right)^{\frac{1}{1+\gamma}} \tag{44}$$

Substituting Eq. (44) into Eq. (43) yields

$$\begin{aligned}\dot{V}_k \leq &-\frac{\lambda_{\min}^{Q}\alpha_k\beta_k N^{1-\gamma}}{p^{-\frac{1}{1+\gamma}}\left(\alpha_k+\frac{\beta_n}{1+\gamma}\right)^{\frac{1}{1+\gamma}}}V_k^{\frac{\gamma}{1+\gamma}}\\ &-\frac{\lambda_{\min}^{Q}\beta_k^2 N^{1-2\gamma}}{p^{-\frac{1}{1+\gamma}}\left(\alpha_k+\frac{\beta_n}{1+\gamma}\right)^{\frac{1}{1+\gamma}}}V_k^{\frac{2\gamma}{1+\gamma}}\end{aligned} \tag{45}$$

Case iv) For $\sum_{i=1}^{N}\left|z_k^i\right|\leq 1$, from Eq. (41) we have

$$\sum_{i=1}^{N}\left|z_k^i\right|\geq\left(\frac{V_k}{\tilde{p}\left(\alpha_k+\frac{\beta_k}{1+\gamma}\right)}\right) \tag{46}$$

Substituting Eq. (46) into Eq. (43) obtains

***Table 1**: Initial position of AUVs.*

Vehicles	Starting positions (m)		Destinations (m)	
	X Position	Y Position	X Position	Y Position
Leader	25	20	37.5	44
AUV1	45	27	39	44
AUV2	45.5	48	40	42
AUV3	6	47.5	39	41
AUV4	5	35	37	41
AUV5	31.5	8	37	42

$$\dot{V}_k \leq -\frac{\lambda_{\min}^{Q}\alpha_k\beta_k N^{1-\gamma}}{\overline{p}\left(\alpha_k+\frac{\beta_k}{1+\gamma}\right)}V_k^{\gamma} - \frac{\lambda_{\min}^{Q}\beta_k^2 N^{1-2\gamma}}{\overline{p}\left(\alpha_k+\frac{\beta_k}{1+\gamma}\right)}V_k^{2\gamma} \tag{47}$$

For case $\gamma < 1$, inductions can be carried out in a similar way. To this end, the main results are summarized in the following theorem.

Theorem 3: The observer gains by satisfying $\gamma > 1$ and $\beta_k > 0$, $\forall\, k = 1, 2, \ldots, n$

$$\alpha_k = \frac{\tilde{p}}{\lambda_{\min}^{Q}},\ \ \forall k = 1, 2, \ldots, n-1 \tag{48}$$

$$\alpha_n = \frac{b_n\overline{u}_0\overline{p}}{\lambda_{\min}^{Q}} \tag{49}$$

The set $S = S_1 \cup S_2 \cup \ldots \cup S_n$ with $S_k = \left\{ z_k \sum_{i=1}^{N} \left|z_k^i\right| \leq 1 \right\}$ is a fixed-time attraction with the setting time bounded by

$$T_0 = \sum_{k=1}^{n} t_k \tag{50}$$

where

$$t_k = \frac{1+\gamma}{\alpha_k N^{1-\gamma} c_k} + \frac{1+\gamma}{\beta_k N^{1-2\gamma} c_k(\gamma-1)} \tag{51}$$

$$c_k = \frac{\lambda_{\min}^{Q_k}\beta_k}{p^{-\frac{1}{1+\gamma}}(\alpha_k+\frac{\beta_k}{1+\gamma})^{\frac{1}{1+\gamma}}} \tag{52}$$

Thus, the observer dynamics are globally asymptotically stable.

***Table 2**: Variation in the AUV positions at different time instants.*

Time (s)	25 s		50 s		75 s		100 s	
Position (m)	X	Y	X	Y	X	Y	X	Y
Leader	30	23	25	36	28	29	26	32
AUV1	37	25	22	33	29	32	27	34
AUV2	24	31	23	28	28	33	29	34
AUV3	37	25	28	26	25	33	27	31
AUV4	19	34	32	30	25	32	29	31
AUV5	30	30	30	35	26	29	30	32

5. RESULTS AND DISCUSSION

The proposed path planner for an MAS with multiple AUVs has been tested by simulation performed using MATLAB. This simulation shows a leader AUV and five follower AUVs. The follower AUVs are represented as AUV1, AUV2, AUV3, AUV4, and AUV5. The starting positions and destinations of the leader and follower (AUV1–AUV5) AUVs are given in Table 1. The corresponding Laplacian matrix L admits the following spectrum: {0; 1.382; 2.382; 3.618; 4.618}. The simulation parameters for the AUV are taken from the experimental values presented in [26].

Figs. 3 to 5 show the positions obtained by all the AUVs at different time instances, such as 25 s, 50 s, and 75 s, respectively. Figs. 4(a) and (b) show the positions obtained by all the AUVs after 50 s and 75 s, respectively. The leader and follower AUVs obtained the desired formation at 100 s as shown in Fig. 5. The detailed positions obtained by the leader and follower AUVs at 25 s, 50 s, 75 s, and 100 s are presented in Table 2.

Fig. 6 shows the paths traced by all AUVs after obtaining the desired shape. Figs. 7 and 8 show the tracking error variations from 0 to 350 s in the X and Y directions, respectively. According to Table 3, the follower AUV tracks the leader AUV in the X and Y directions from 0 to 50 s. After 30 s, as can be observed, the follower AUVs do not track the leader AUV but try to follow its path. By magnifying both the figures, all AUVs can be seen to follow the path in formation after 40 s until they reach their destination. The errors in both the X and Y axis are uniform which proves that the proposed controller is stable and uniform.

Another approach may be proposed using the reference path as the sinusoidal path. The initial positions for the follower agents are given as $\eta_1(0) = [-70,\ -200]^T$, $\eta_2(0) = [-25,\ 250]^T$, $\eta_3(0) = [-20,\ 270]^T$, $\eta_4(0) = [-50,\ 124]^T$, and $\eta_5(0) = [-100,\ 300]^T$.

The formation achieved by tracking the trajectory of the desired virtual leader's path with five agent followers, as shown in Figs. 9, 10, and 11, represents the error generated by the x and y coordinates of cooperatively coordinated AUVs. From Figs. 10 and 11, it can be observed that the follower AUVs track the leader AUV after 20 s until reaching the destination point. As can

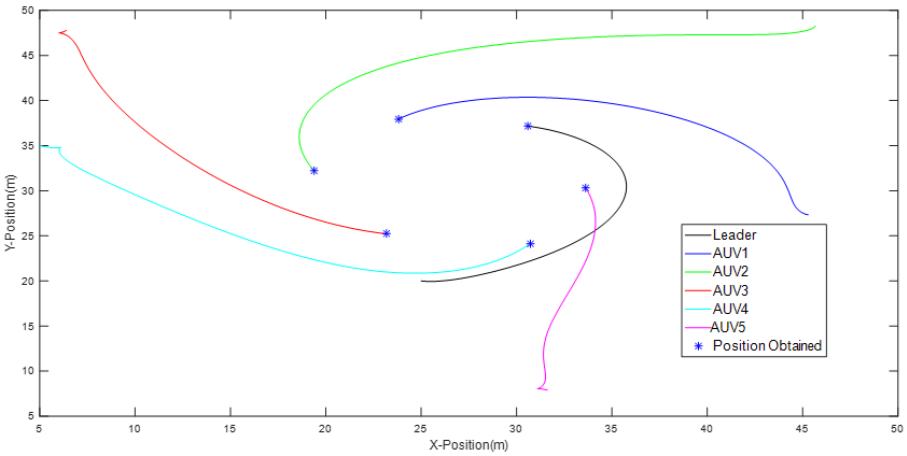

***Fig. 3**: Positions of AUVs after obtaining desired formation shape after 25 s.*

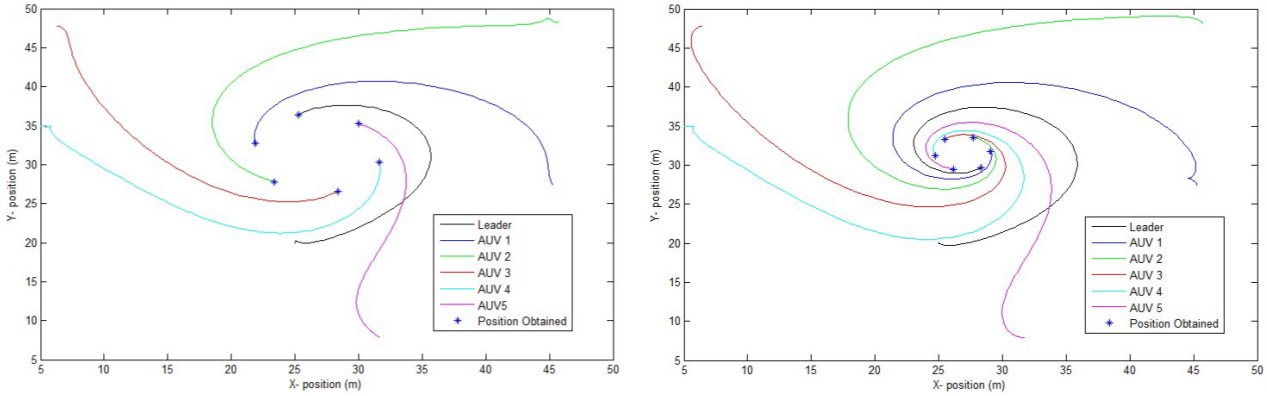

(a) *(b)*

***Fig. 4**: Positions of the AUVs after (a) 50 s and (b) 75 s.*

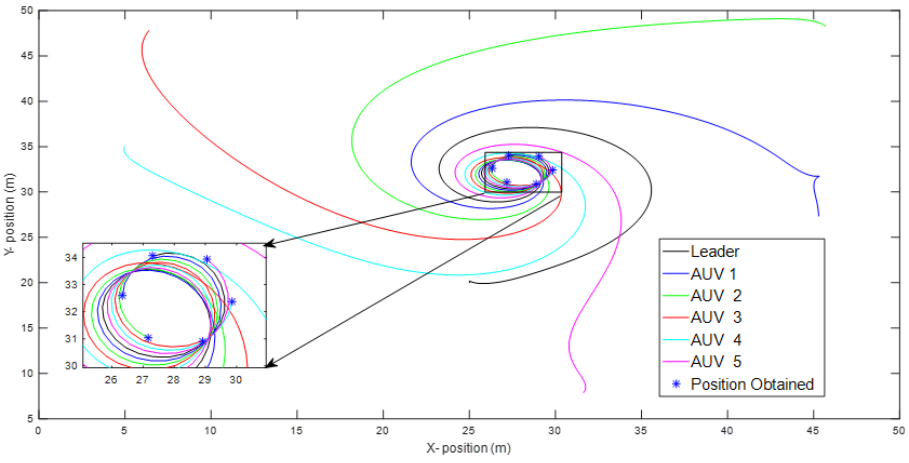

***Fig. 5**: Positions of the AUVs obtained after 100 s.*

be observed, the position errors converge to zero, i.e., the follower and desired states of the leader AUV are closely matched. The errors in both the X and Y axis are uniform, proving that the proposed controller is stable and uniform after 20 s.

6. CONCLUSION

In this paper, a bio-inspired multi-agent system (MAS) is employed to address the personal path planning problem encountered when navigating a team of AUVs toward their destination. Each AUV is designated as an agent, connected by the communication network

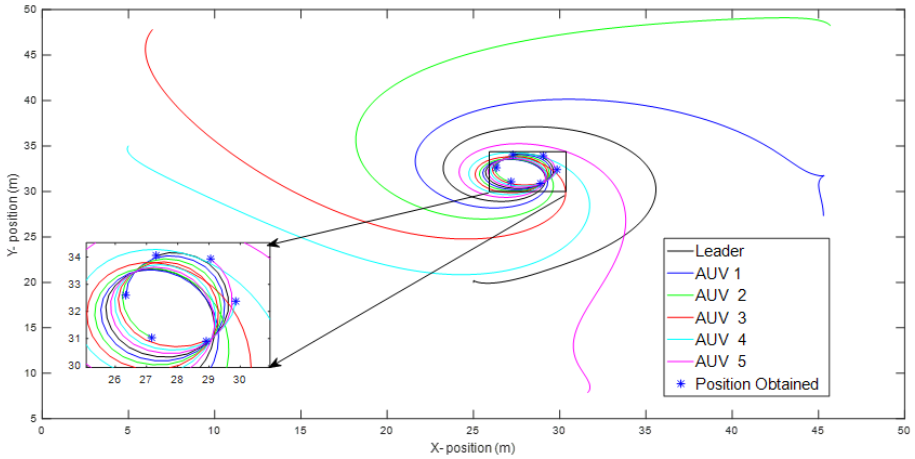

***Fig. 6**: Complete paths of the AUVs after reaching their destination.*

***Table 3**: Variation of the tracking error in X and Y directions.*

Time (s)	0		10		20		30		40		50	
Tracking error (m)	X	Y	X	Y	X	Y	X	Y	X	Y	X	Y
Leader	21	7	15	11	−4	8	−3	−4	−2	0.1	1.3	1.5
AUV1	20	28	6	27	−16	7	−1	−9	−2.5	−1.5	1	3
AUV2	−19	27.7	−22	23	−19	−4	4	−10	−2	−3	−0.6	3.5
AUV3	−19	27.7	−22	23	−19	−4	4	−10	−2	−3	−0.6	3.5
AUV4	−20	15	−18	7.5	−10	−12.5	7	−6	−0.8	−3.5	−2	2.5
AUV5	6	−12	0.3	−10	−2	−11	5	−1	1	−2	−1.6	0.6

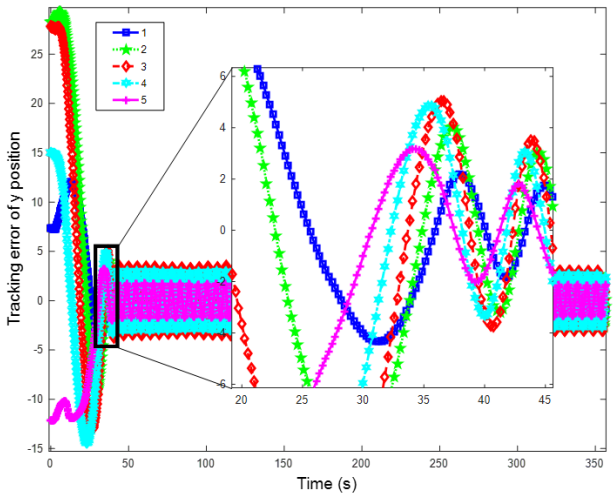

***Fig. 7**: Tracking error in the X direction.*

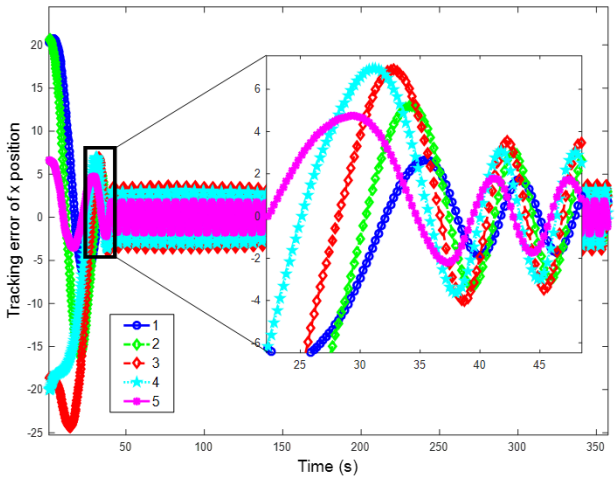

***Fig. 8**: Tracking error in the Y direction.*

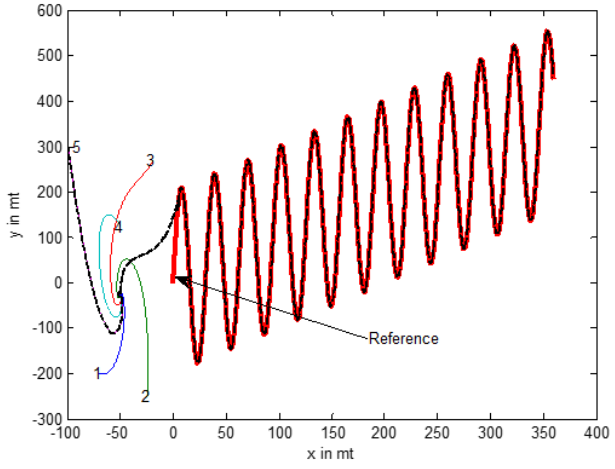

***Fig. 9**: Trajectory tracking of the reference path for five agents following the virtual leader.*

and assuming full communication. The agent AUVs are identical and estimate the relative position of their neighbor AUVs while moving toward their respective destinations. The proposed multi-AUV system comprises a leader AUV and five follower AUVs. The proposed MAS implements a DPC algorithm to maintain coordination and a safe distance among agent AUVs by imposing the distance constraint. The agents switch from one state to another and progress over time until the desired coordinated shape is obtained. The same is then

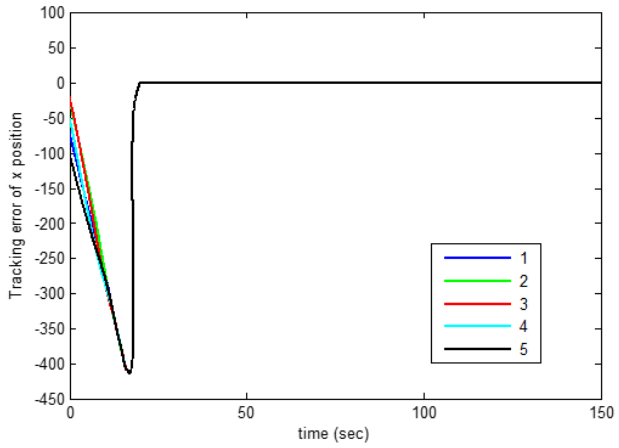

***Fig. 10**: Tracking error in the x position.*

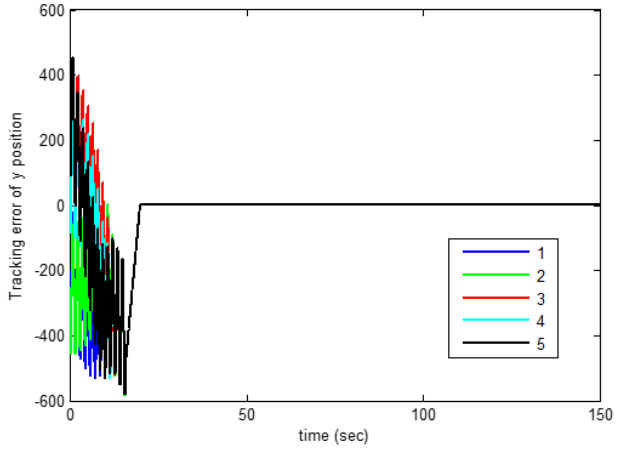

***Fig. 11**: Tracking error in the y position.*

maintained by the agent AUVs while moving toward their individual program. The simulation results verify that the proposed method is successful in coordinating path planning for the multi-AUV system. The proposed bio-inspired multi-AUV system can be used to discover unknown underwater terrains, for surveillance of the seabed and to access unreachable underwater areas.

ACKNOWLEDGMENTS

This work is supported by the Seed Funding Research Project under OURIIP – 2021 under Odisha State Higher Education Council (OSHEC), who have been supportive and worked actively to provide us with the protected academic time to pursue those goals.

REFERENCES

[1] T. I. Fossen, *Guidance and Control of Ocean Vehicles*. Chichester, UK: John Wiley & Sons, 1994, pp. 6–54.

[2] L. Durica, B. Micieta, P. Bubenik, and V. Binasova, "Manufacturing multi-agent system with bio-inspired techniques: CODESA-prime," *MM Science Journal*, vol. 2015, pp. 829–837, Dec. 2015.

[3] B. Das, B. Subudhi, and B. B. Pati, "Formation control of underwater vehicles using multi agent system," *Archives of Control Sciences*, vol. 30, no. 2, pp. 365–384, 2020.

[4] Y. Deng, P.-P. J. Beaujean, E. An, and E. Carlson, "Task allocation and path planning for collaborative autonomous underwater vehicles operating through an underwater acoustic network," *Journal of Robotics*, vol. 2013, 2013, Art. no. 483095.

[5] B. Das, B. Subudhi, and B. B. Pati, "Employing nonlinear observer for formation control of AUVs under communication constraints," *International Journal of Intelligent Unmanned Systems*, vol. 3, no. 2/3, pp. 122–155, 2015.

[6] B. Das, B. Subudhi, and B. B. Pati, "Co-operative control of a team of autonomous underwater vehicles in an obstacle-rich environment," *Journal of Marine Engineering & Technology*, vol. 15, no. 3, pp. 135–151, 2016.

[7] B. Das, B. Subudhi, and B. B. Pati, "Co-operative control coordination of a team of underwater vehicles with communication constraints," *Transactions of the Institute of Measurement and Control*, vol. 38, no. 4, pp. 463–481, Apr. 2016.

[8] Z. Zuo, M. Defoort, B. Tian, and Z. Ding, "Distributed consensus observer for multiagent systems with high-order integrator dynamics," *IEEE Transactions on Automatic Control*, vol. 65, no. 4, pp. 1771–1778, Apr. 2020.

[9] M. Chen and D. Zhu, "A workload balanced algorithm for task assignment and path planning of inhomogeneous autonomous underwater vehicle system," *IEEE Transactions on Cognitive and Developmental Systems*, vol. 11, no. 4, pp. 483–493, Dec. 2019.

[10] S. Ul'yanov and N. Maksimkin, "Software toolbox for analysis and design of nonlinear control systems and its application to multi-AUV path-following control," in *2017 40th International Convention on Information and Communication Technology, Electronics and Microelectronics (MIPRO)*, 2017, pp. 1032–1037.

[11] R. Olfati-Saber, J. A. Fax, and R. M. Murray, "Consensus and cooperation in networked multi-agent systems," *Proceedings of the IEEE*, vol. 95, no. 1, pp. 215–233, Jan. 2007.

[12] P. Szymak and T. Praczyk, "Control systems of underwater vehicles in multi-agent system of underwater inspection," in *Proceedings of the 11th WSEAS international conference on automatic control, modelling and simulation (ACMOS'09)*, 2009, pp. 153–156.

[13] H. Yang and F. Zhang, "Geometric formation control for autonomous underwater vehicles," in *2010 IEEE International Conference on Robotics and Automation*, 2010, pp. 4288–4293.

[14] X. Q. Bian, T. Chen, J. Zhou, and Z. Yan, "Research of autonomous control based on multi-agent for AUV," in *2009 International Workshop on Intelligent Systems*

and Applications, 2009.

[15] Z. Hu, C. Ma, L. Zhang, A. Halme, T. Hayat, and B. Ahmad, "Formation control of impulsive networked autonomous underwater vehicles under fixed and switching topologies," *Neurocomputing*, vol. 147, pp. 291–298, Jan. 2015.

[16] C. Viel, "Control law and state estimators design for multi-agent system with reduction of communications by event-triggered approach," Ph.D. dissertation, Automatic Control Engineering, Université Paris-Saclay, Paris, France, 2017.

[17] M. R. Bharamagoudra, S. S. Manvi, and B. Gonen, "Event driven energy depth and channel aware routing for underwater acoustic sensor networks: Agent oriented clustering based approach," *Computers & Electrical Engineering*, vol. 58, pp. 1–19, Feb. 2017.

[18] Z. Gallehdari, N. Meskin, and K. Khorasani, "Distributed reconfigurable control strategies for switching topology networked multi-agent systems," *ISA Transactions*, vol. 71, pp. 51–67, Nov. 2017.

[19] R. Jurdak, A. Elfes, B. Kusy, A. Tews, W. Hu, E. Hernandez, N. Kottege, and P. Sikka, "Autonomous surveillance for biosecurity," *Trends in Biotechnology*, vol. 33, no. 4, pp. 201–207, Apr. 2015.

[20] H. G. de Marina, M. Cao, and B. Jayawardhana, "Controlling rigid formations of mobile agents under inconsistent measurements," *IEEE Transactions on Robotics*, vol. 31, no. 1, pp. 31–39, Feb. 2015.

[21] J. Fu and J. Wang, "Fixed-time coordinated tracking for second-order multi-agent systems with bounded input uncertainties," *Systems & Control Letters*, vol. 93, pp. 1–12, Jul. 2016.

[22] S. Bhattacharya, M. Likhachev, and V. Kumar, "Distributed path consensus algorithm," University of Pennsylvania, Philadelphia, PA, USA, Technical report. MS-CIS-10-07, 2010.

[23] S. Bhattacharya, M. Likhachev, and V. Kumar, "Multi-agent path planning with multiple tasks and distance constraints," in *2010 IEEE International Conference on Robotics and Automation*, 2010, pp. 953–959.

[24] M. K. Rizwan, B. Das, and B. B. Pati, "A criterion based adaptive RSIC scheme in underwater communication," *Journal of Systems Engineering and Electronics*, vol. 32, no. 2, pp. 408–416, Apr. 2021.

[25] B. Das, B. Subudhi, and B. B. Pati, "Cooperative formation control of autonomous underwater vehicles: An overview," *International Journal of Automation and Computing*, vol. 13, no. 3, pp. 199–225, Jun. 2016.

[26] B. Das, B. Subudhi, and B. B. Pati, "Adaptive sliding mode formation control of multiple underwater robots," *Archives of Control Sciences*, vol. 24, no. 4, pp. 515–543, Dec. 2014.

Sarada Prasanna Sahoo received his B. Tech. degree in Electrical Engineering department from Utkal University, Bhubaneswar, India in 2006 and M. Tech. degree in Power Control and Drives specialisation from National Institute of Technology, Rourkela, India in 2010. Currently, he is pursuing Ph.D. degree in Electrical Engineering department from Veer Surendra Sai University of Technology Burla, Odisha, India. His research interests include Control of Autonomous Underwater Vehicle and Control application to Electric Drives.

Bikramaditya Das received his B.Tech. degree in Electronics and Telecommunications Engineering from the Biju Patnaik University of Technology, Rourkela, India, M Tech. degree in Wireless Communication from Department of Electrical Engineering, National Institute of Technology Rourkela, India in 2010, and the Ph.D. degree in control under communication constraints from Department of Electrical Engineering, Veer Surendra Sai University of Technology Odisha, Burla, India, in 2016. He is currently working as Assistant Professor at Department of Electronics and Telecommunication Engineering, Veer Surendra Sai University of Technology Odisha, Burla, India. He is an associate member of IEI. His research interests include formation control of autonomous underwater vehicles, robotics and wireless communication.

Bibhuti Bhusan Pati is currently working as a Professor in the Department of Electrical Engineering, Veer Surendra Sai University of Technology Odisha, Burla, India. He is the fellow of Institution of Engineers, member Indian Society for Technical Education, Bigyan Academy, and Engineering Congress. He has published more than 180 papers in reputed journals and conferences. He is the investigator of many AICTE sponsored projects. His research of interests includes control system and applications to power system.